DOI: 10.1534/genetics.110.113944

Feed-Forward Regulation of a Cell Fate Determinant by an RNA-Binding Protein Generates Asymmetry in Yeast

Joshua J. Wolf,* Robin D. Dowell,†,[2] Shaun Mahony,† Michal Rabani,† David K. Gifford† and Gerald R. Fink*,[1]

*Whitehead Institute for Biomedical Research, Massachusetts Institute of Technology, Cambridge, Massachusetts 02142 and †Computer Science and Artificial Intelligence Laboratory. Massachusetts Institute of Technology, Cambridge, Massachusetts 02139

Manuscript received January 11, 2010
Accepted for publication April 7, 2010

ABSTRACT

Saccharomyces cerevisiae can divide asymmetrically so that the mother and daughter cells have different fates. We show that the RNA-binding protein Khd1 regulates asymmetric expression of *FLO11* to determine daughter cell fate during filamentous growth. Khd1 represses transcription of *FLO11* indirectly through its regulation of *ASH1* mRNA. Khd1 also represses *FLO11* through a post-transcriptional mechanism independent of *ASH1*. Cross-linking immunoprecipitation (CLIP) coupled with high-throughput sequencing shows that Khd1 directly binds repetitive sequences in *FLO11* mRNA. Khd1 inhibits translation through this interaction, establishing feed-forward repression of *FLO11*. This regulation enables changes in *FLO11* expression between mother and daughter cells, which establishes the asymmetry required for the developmental transition between yeast form and filamentous growth.

ASYMMETRIC cell division produces two cells with different developmental fates (Horvitz and Herskowitz 1992). The unequal inheritance of cell fate determinants establishes this asymmetry in many systems through diverse mechanisms that ultimately produce asymmetric gene expression between cells (Macara and Mili 2008). In multicellular eukaryotes, this process directs a cell lineage down a developmental path. In *Saccharomyces cerevisiae,* each mitotic division requires a new decision to determine the fate of the daughter cell, providing a tractable model to study the underlying mechanisms of asymmetric cell division.

The RNA-binding protein Khd1 (KH-domain protein 1) regulates the asymmetric expression of *ASH1* in budding yeast to control mating-type switching, a key developmental event in haploid cells (Irie *et al.* 2002; Paquin *et al.* 2007; Hasegawa *et al.* 2008). Ash1 protein accumulates specifically in the nuclei of daughter cells (Bobola *et al.* 1996; Sil and Herskowitz 1996). Genetic and biochemical analysis led to the model that Khd1 represses translation of *ASH1* mRNA during transport to the bud tip, where phosphorylation by Yck1 reduces the affinity of Khd1 for the transcript, relieving repression and allowing translation to occur (Long *et al.* 1997; Chartrand *et al.* 2002; Irie *et al.* 2002; Paquin *et al.* 2007). As Ash1 is a transcription factor that represses mating-type switching, translational repression of *ASH1* mRNA in the mother but not the daughter leads to asymmetry—the mother can switch mating type, but the daughter cannot (Strathern and Herskowitz 1979; Chartrand *et al.* 2002; Paquin and Chartrand 2008).

ASH1 has also been implicated in the regulation of filamentous growth, another developmental event in *S. cerevisiae* (Chandarlapaty and Errede 1998). Under conditions of nitrogen starvation, diploid cells enact a specialized growth program characterized by an elongated morphology and unipolar budding that leads to the formation of filaments (Gimeno *et al.* 1992). The transition to filamentous growth requires an asymmetric cell division, as a yeast-form mother cell produces a filamentous daughter cell. *ASH1* regulates filamentous growth by activating expression of *FLO11* (Pan and Heitman 2000), which encodes a cell wall protein required for this growth form (Lambrechts *et al.* 1996; Lo and Dranginis 1998). Cells induce *FLO11* expression to activate filamentation in response to nitrogen starvation (Lo and Dranginis 1998). Deletion of *ASH1* prevents both *FLO11* expression (Pan and Heitman 2000) and the transition to filamentous growth (Chandarlapaty and Errede 1998).

Khd1 has no known role in regulating filamentous growth. However, since Khd1 represses *ASH1* in the context of mating-type switching, it may regulate *ASH1* during filamentation as well. Given that RNA-binding

Supporting information available online at http://www.genetics.org/cgi/content/full/genetics.110.113944/DC1.

Sequence data from this article have been deposited with the Sequence Read Archive under accession no. SRA012416.

[1]*Corresponding author:* Gerald R. Fink, Whitehead Institute for Biomedical Research, MIT, 9 Cambridge Center, Cambridge, MA 02142. E-mail: gfink@wi.mit.edu

[2]*Present address:* Molecular, Cellular, and Developmental Biology, 347 UCB, University of Colorado, Boulder, CO 80309

proteins can coordinate the expression of mRNAs encoding functionally related proteins (Keene 2007), Khd1 may regulate additional genes in the filamentation pathway. Microarray analysis following immunoprecipitation of Khd1 has been used to identify its mRNA targets (Hasegawa *et al.* 2008; Hogan *et al.* 2008), but the strains used do not transcribe *FLO11* mRNA (Liu *et al.* 1996) and the binding of Khd1 to mRNAs of the filamentation pathway such as *FLO11* would not have been detected.

The ability to comprehensively define post-transcriptional regulatory networks has been enormously advanced by the cross-linking immunoprecipitation (CLIP) method. CLIP utilizes UV radiation to crosslink an RNA-binding protein to its direct RNA targets *in vivo,* providing a snapshot of binding interactions. Direct sequencing of the RNAs following RNAse treatment localizing binding sites to a 60- to 100-nucleotide region within target transcripts (Ule *et al.* 2003). CLIP has been used in combination with high-throughput sequencing to comprehensively identify RNA targets of mammalian RNA-binding proteins (Licatalosi *et al.* 2008; Sanford *et al.* 2009; Yeo *et al.* 2009), but has not been previously applied to yeast.

In this report, we use genetic analysis and CLIP coupled with high-throughput sequencing to determine the role of Khd1 in regulating filamentous growth. We find that Khd1 regulates both transcription and translation of *FLO11* to repress filamentation. Khd1 represses *FLO11* at the transcriptional level through its inhibition of *ASH1*, as we predicted based on published regulatory interactions (Chandarlapaty and Errede 1998; Pan and Heitman 2000; Irie *et al.* 2002; Paquin *et al.* 2007; Hasegawa *et al.* 2008), and at the post-transcriptional level by directly repressing translation of *FLO11* mRNA. The feed-forward regulation of *FLO11* by Khd1 provides a dynamic mechanism for generating asymmetric expression and determining daughter cell fate following cell division. *FLO11* mRNA is the predominant unique transcript bound by Khd1, indicating that this regulation is a primary function of the protein. Khd1 binds to repeated sequences in the coding region of *FLO11* mRNA and mRNAs encoding many other cell surface proteins, suggesting that this RNA binding protein may coordinate the synthesis of many disparate proteins that assemble into the cell wall.

MATERIALS AND METHODS

Yeast strains, media, and growth conditions: All yeast strains used in this study are derived from Σ1278b and listed in supporting information, Table S1. Standard yeast media, yeast transformations, and genetic manipulations were performed as previously described (Guthrie and Fink 2001). To induce filamentation, strains were grown on nitrogen-poor SLAD media (Gimeno *et al.* 1992). Approximately 20 cells per strain were spotted onto a SLAD plate in 50 μl of water to compare filamentation under comparable conditions. To assay agar adhesion, 10^6 cells were spotted onto a YPD plate in 5 μl and grown for 3 days at 30° prior to washing. Yeast strains carrying gene deletions were constructed by PCR amplification of kanamycin-resistance gene cassettes from the yeast deletion library (Winzeler *et al.* 1999) with approximately 200 bases of flanking sequence and transformation into Σ1278b. Yeast strains carrying TAP-tagged Khd1 were similarly constructed by PCR amplification of the *KHD1-TAP::HIS3* construct from the TAP-tag library (Ghaemmaghami *et al.* 2003) and transformation into Σ1278b. Strains carrying P_{ADH} or P_{CYC1} (Janke *et al.* 2004) were constructed by PCR amplification with primers containing 50 bp of homology to the target locus and transformation into Σ1278b. Strains carrying *GFP::ADH 3′ UTR::URA3* or *ADH 3′ UTR::URA3* were similarly constructed using a plasmid provided by Sherwin Chan. See Table S2 for primer sequences.

Plasmid construction: The Khd1 overexpression construct was made by amplifying the gene using PCR, with oligonucleotides that added restriction sites (*Not*I at the 5′ end, *Xho*I at the 3′ end) to the final product (Table S2). Amplified DNA was digested using *Not*I and *Xho*I and cloned into p413TEF (Mumberg *et al.* 1995).

Flow cytometry and immunofluoresence: Single colonies were picked after 2 days of growth on YPD plates and resuspended in 1.5 ml liquid YPD. Cells were inoculated into 10 ml liquid YPD and grown for 18 hr to OD_{600} 0.13–0.16, washed twice with PBS, and resuspended in 50 μl PBS containing 1 μl Alexafluor 488-conjugated anti-hemaglutinin antibody (Molecular Probes A-21287) per 200 μl PBS. Cells were incubated 30 min at 4° and washed three times in PBS prior to flow cytometry using the BD FACSCalibur, or imaging with the Nikon Eclipse TE2000-S.

qPCR: Total RNA was obtained by standard acid phenol extraction from 1 ml of cultures grown to OD_{600} 0.9–1.1 in YPD. The Qiagen QuantiTect Reverse Transcription Kit was used to remove residual genomic DNA and reverse transcribe the RNA templates to generate cDNAs. Aliquots of cDNA were used in Real Time PCR analyses with reagents from Applied Biosystems and the ABI 7500 real-time PCR system.

Immunoprecipitation for measuring RNA enrichment: TAP tag immunoprecipitation and RNA isolation was performed as previously described (Gerber *et al.* 2004), using 200 ml of starting culture rather than 1 liter and proportionately fewer reagents.

Cross-linking immunoprecipitation: Khd1–TAP was purified from 1 liter of cells grown to OD_{600} 2.5 and UV crosslinked three times at 400 mJ/cm^2. Purification using calmodulin sepharose was followed by binding to magnetic IgG beads (File S1). The CLIP protocol was then followed as previously described (Ule *et al.* 2005). The resulting cDNA was amplified using PCR with oligonucleotides containing sequences for hybridization to the Illumina flow cell (Table S2).

Illumina sequencing: Samples were sequenced using Illumina sequencing with a custom primer (Table S2), returning 16,026,920 36-nucleotide-long reads. Reads containing unresolved bases (*N*) were ignored. The complete set of reads contained 6,324,854 unique sequences. All reads were mapped to the Σ1278b genome (Dowell *et al.* 2010) using Novoalign (v1.05; second September 2008) with default settings. All mappings are included, weighted inversely by the number of genomic locations to which a read maps. The reads have been deposited in the Sequence Read Archive under accession no. SRA012416.

Peak calling: The peak caller uses a rolling window approach (10-base windows; 5-base offset) to compare the observed reads to those expected from a Poisson background model. Adjacent enriched windows are combined into peaks. Peaks are assigned to genes on the basis of overlap with

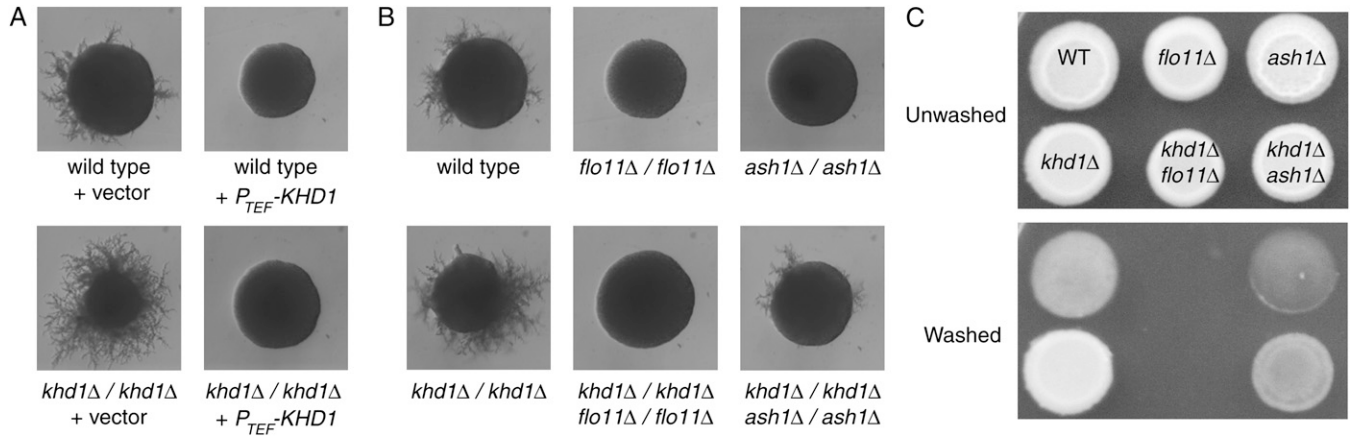

Figure 1.—Khd1 represses *FLO11*-dependent phenotypes independent of *ASH1*. (A) Khd1 represses filamentous growth in diploid cells. P_{TEF}–*KHD1* is an overexpression construct. (B) Khd1 represses filamentation independent of *ASH1*. (C) *ASH1*-independent repression of haploid agar adhesion by Khd1. Picture taken of the same plate before and after washing.

existing annotation, extending 500 nucleotides in each direction (unless the extension overlaps adjacent annotation) to account for UTRs.

A local (5 kb) window is used to parameterize the background model. A visual examination of the read mappings relative to available tiled expression data (Danford *et al.* 2010) indicates that reads are strand specific and show perfect correspondence with expressed segments, indicating the background of possible RNA binding sites is the transcriptome, not the genome. A weak correlation is observed between the expression levels of a transcript and the number of observed reads.

We set a peak cutoff by maximizing the correspondence of gene targets predicted relative to the targets reported by Hasegawa *et al.* (2008). The peaks are weighted by the corresponding expression level of each transcript, as determined from tiled expression data (Danford *et al.* 2010). Only peaks containing at least 50% of the reads of the transcript's maximal peak size are considered.

Motif discovery: Three methods were utilized to identify the motif recognized by Khd1. First, MEME (v4.1; Bailey and Elkan 1994) was utilized on the sequences under the peaks, filtering to remove highly identical sequences (80% identity). Second, all *k*-mers were evaluated (for $k = 1, 2, 3, 4$) to identify overrepresented sequences under the peaks. Random non-peak windows of matching length were selected from the same set of transcripts as the peaks to calculate the distribution of background *k*-mers. Finally, "RNApromo" (Rabani *et al.* 2008) and CMfinder (Yao *et al.* 2006) were applied to the peaks to search for potential secondary structure. The structure motifs returned were single-strand loops with sequence patterns consistent with the primary sequence motif identified by MEME. Presence of the discovered MEME motif within the peak list was determined using MAST (v4.1; Bailey and Gribskov 1998) with default parameters.

Western blot analysis: Protein was prepared using TCA precipitation from 3 ml of culture grown to OD_{600} of 0.9–1.1, resuspended in 150 μl SDS loading buffer, and boiled for 10 min. Ten microliters were run on a 10% SDS–polyacrylamide gel and transferred to nitrocellulose filter paper. Blotting against GFP was performed with mouse anti-GFP primary antibody (Roche 11814460001) and HRP-conjugated sheep anti-mouse secondary antibody (Amersham NA931V), and against tubulin using rat anti-tubulin (Accurate Chemicals MCA77G) and HRP-conjugated goat anti-rat antibody (Jackson ImmunoResearch 112-035-062). Blots were detected using SuperSignal West femto substrate (Thermo Scientific 34095).

RESULTS

Khd1 has *ASH1*-dependent and *ASH1*-independent functions in repressing *FLO11*: Given that *ASH1* promotes filamentous growth (Chandarlapaty and Errede 1998) by activating transcription of *FLO11* (Pan and Heitman 2000) and that Khd1 represses *ASH1* in the context of mating-type switching (Irie *et al.* 2002; Paquin *et al.* 2007; Hasegawa *et al.* 2008), we hypothesized that Khd1 regulates filamentous growth. Genetic analysis shows that Khd1 represses filamentation. The *khd1*Δ/*khd1*Δ mutant is hyperfilamentous relative to wild type, and cells fail to filament when Khd1 is overexpressed (Figure 1A). The hyperfilamentation phenotype of the *khd1*Δ/*khd1*Δ mutant requires *FLO11*. As is the case with the *flo11*Δ/*flo11*Δ mutant, the *khd1*Δ/*khd1*Δ *flo11*Δ/*flo11*Δ mutant is nonfilamentous (Figure 1B). These findings are consistent with our prediction that Khd1 regulates filamentation by repressing transcription of *FLO11* indirectly through its translational repression of *ASH1* mRNA.

However, Khd1 represses filamentation at least in part through an *ASH1*-independent pathway. The *khd1*Δ/*khd1*Δ *ash1*Δ/*ash1*Δ double mutant is filamentous, unlike the *ash1*Δ/*ash1*Δ single mutant, indicating that Khd1 represses filamentation independent of *ASH1* (Figure 1B). This finding extends to haploid agar adhesion, another *FLO11*-dependent phenotype. Cells deleted for *KHD1* adhere more than wild-type cells, and *khd1*Δ *ash1*Δ double mutants adhere more than *ash1*Δ single mutants (Figure 1C). As is the case for filamentation, adhesion of both wild-type and *khd1*Δ cells requires *FLO11* (Figure 1C; Lambrechts *et al.* 1996; Lo and Dranginis 1998). These data show that Khd1 represses *FLO11*-dependent phenotypes independent of *ASH1*.

TABLE 1

Khd1 represses Flo11 protein expression independent of *ASH1*

Strain	% cells expressing Flo11	Mean expression in Flo11 positive cells
Wild type	58 ± 6	100 ± 13
*khd1*Δ/*khd1*Δ	80 ± 4	153 ± 18
*ash1*Δ/*ash1*Δ	14 ± 2	56 ± 3
*khd1*Δ/*khd1*Δ *ash1*Δ/*ash1*Δ	32 ± 5	61 ± 5

Values are average of four independent trials. Error reported as standard deviation.

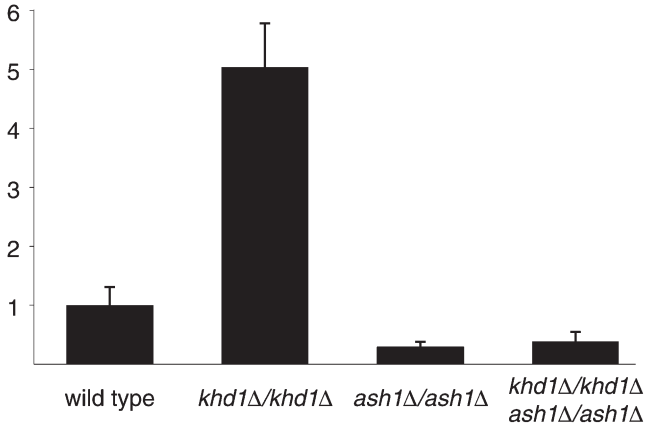

Figure 2.—Khd1 represses *FLO11* mRNA levels through *ASH1*. *FLO11* mRNA levels normalized to *ACT1* mRNA. Values are average of four independent experiments. Error reported as standard deviation.

Given the repression of *FLO11*-dependent phenotypes by Khd1, we tested whether Khd1 regulates *FLO11* expression. To quantify *FLO11* expression, we employed a *FLO11::HA* allele that permits the measurement of Flo11 protein in individual cells (Guo *et al.* 2000). Flo11 protein is expressed in a subset of cells in a clonal population because of variegating transcription from the *FLO11* promoter (Halme *et al.* 2004; Bumgarner *et al.* 2009). Mutations that affect *FLO11* mRNA levels and filamentation show a corresponding change in the number of cells containing the *FLO11::HA* allele that stain positive using an anti-HA antibody (Halme *et al.* 2004).

Flow cytometry shows that Khd1 represses Flo11 protein expression. Deletion of *KHD1* increases the percentage of diploid cells expressing Flo11 protein (Table 1). In addition, the *khd1*Δ/*khd1*Δ cells that express Flo11 protein do so at a higher level than wild-type cells that express Flo11. Similar to its regulation of filamentous growth, Khd1 represses Flo11 protein expression independent of *ASH1*. Although the populations of *khd1*Δ/*khd1*Δ *ash1*Δ/*ash1*Δ and *ash1*Δ/*ash1*Δ cells that express Flo11 display similar levels of the protein, a higher percentage of *khd1*Δ/*khd1*Δ *ash1*Δ/*ash1*Δ cells express Flo11 (Table 1). The Flo11 expression data, together with the filamentation and agar adhesion phenotypes, point to an *ASH1*-independent function for Khd1 in repressing *FLO11*.

To explore the regulation of *FLO11* by Khd1, we used qPCR to measure *FLO11* mRNA levels. *khd1*Δ/*khd1*Δ mutants have increased *FLO11* mRNA levels relative to wild type (Figure 2), which indicates that Khd1 represses *FLO11* mRNA accumulation. In contrast to its *ASH1*-independent repression of filamentation and Flo11 protein expression, Khd1 represses *FLO11* mRNA levels exclusively through its regulation of *ASH1*. *khd1*Δ/*khd1*Δ *ash1*Δ/*ash1*Δ double mutants display the same *FLO11* mRNA levels as *ash1*Δ/*ash1*Δ single mutants, which are below that of wild type (Figure 2). We conclude that Khd1 represses transcription of *FLO11* mRNA through its regulation of *ASH1*. The restoration of filamentation and increased Flo11 protein expression in *khd1*Δ/*khd1*Δ *ash1*Δ/*ash1*Δ relative to *ash1*Δ/*ash1*Δ, without a concomitant increase in *FLO11* mRNA levels, suggests that Khd1 represses *FLO11* through a post-transcriptional mechanism as well.

Khd1 binds repeated sequences in the *FLO11* open reading frame: The post-transcriptional regulation of *FLO11* by Khd1 suggested that Khd1 might interact with *FLO11* mRNA. To address this possibility, we tested whether *FLO11* mRNA co-immunoprecipitates with a TAP-tagged version of Khd1. qPCR shows that immunoprecipitation of Khd1–TAP enriches *FLO11* mRNA more than 50-fold (Figure 3A). The same immunoprecipitation does not enrich *FLO11* mRNA when Khd1 is untagged. Immunoprecipitations testing for an interaction between Khd1 and constructs containing different combinations of the *FLO11* open reading frame and untranslated regions indicate that Khd1 interacts with the *FLO11* coding sequence (Figure S1).

To examine the interaction between Khd1 and *FLO11* mRNA further, we identified *in vivo* RNA binding sites for Khd1 using CLIP in conjunction with high-throughput sequencing (File S2, Figure S2, and Table S3). The CLIP analysis shows that Khd1 interacts directly with repetitive sequences in *FLO11* mRNA (Figure 3B). *FLO11* mRNA is the most frequently represented unique mRNA in the data set; of the 16 million sequences we generated, 1.97 million derive from Khd1 binding to *FLO11* mRNA.

To determine whether the repeated sequences in *FLO11* mRNA are sufficient for recognition by Khd1, we generated a construct that isolates the *FLO11* repetitive element. Immunoprecipitation of Khd1–TAP enriches a transcript with the *FLO11* repeats fused to *GFP* driven by the *ADH* promoter (Figure 3C). Because the repeats cause a 10-fold decrease in *GFP* mRNA levels relative to the *ADH* promoter driving *GFP* alone (Figure S3), we used the weaker *CYC1* promoter to express comparable

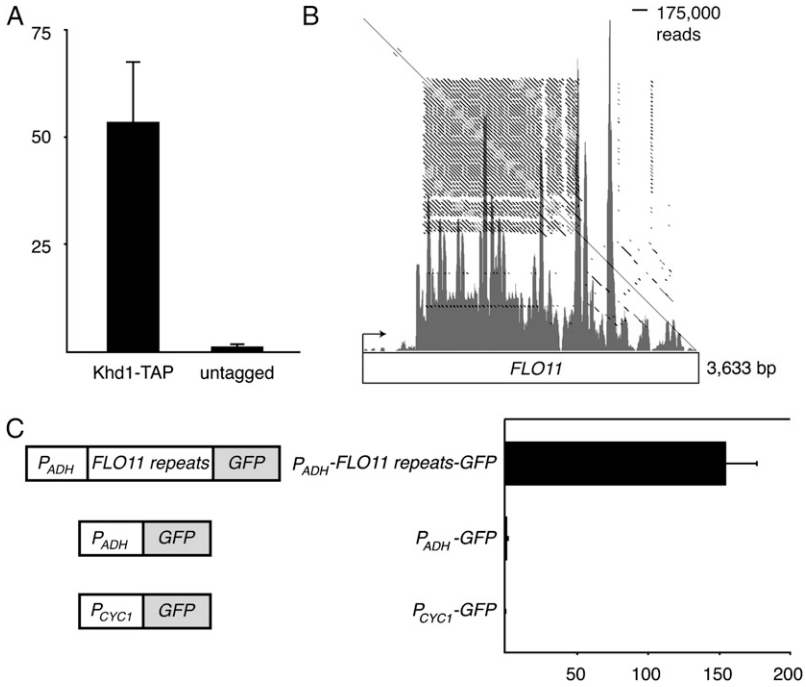

FIGURE 3.—Khd1 binds repetitive sequences in the *FLO11* open reading frame. (A) Enrichment of *FLO11* mRNA following immunoprecipitation from cells expressing either Khd1–TAP or untagged Khd1. (B) Khd1 target sequences from CLIP map to the *FLO11* repetitive element. Histogram of read mappings overlaid on a dot plot highlighting the repetitive region of the *FLO11* open reading frame from the ∑1278b genome (http://www.vivo.colostate.edu/molkit/dnadot/, window size = 11, mismatch limit = 1). (C) Enrichment of constructs following immunoprecipitation of Khd1–TAP. Enrichments expressed as the level of the transcript relative to *ACT1* mRNA in the immunoprecipitate divided by the level of the transcript relative to *ACT1* mRNA in the input. Values are average of four independent experiments. Error reported as standard deviation.

levels of *GFP* without the repeated sequences. *GFP* mRNA does not enrich in the Khd1–TAP immunoprecipitation when driven by either promoter in the absence of the *FLO11* repetitive element (Figure 3C). We conclude that the repeated sequences in *FLO11* mRNA are sufficient for recognition by Khd1.

Khd1 represses translation through the *FLO11* repetitive element: We used the construct with *GFP* fused to the *FLO11* repetitive element to test the effect of Khd1 binding to this region. Western blotting shows that GFP protein levels from this fusion construct increase 12-fold in *khd1*Δ relative to wild type (Figure 4A, compare lanes 1 and 2). qPCR measurements show that Khd1 expression causes a 2-fold decrease in mRNA levels from this construct (Figure 4B compare lanes 1 and 2). We attribute the remaining 6-fold difference in GFP protein levels relative to *GFP* mRNA levels between wild type and *khd1*Δ to translational repression that results from Khd1 binding the *FLO11* repetitive element. Khd1 overexpression further represses the construct with the *FLO11* repeats fused to *GFP*, reducing the amount of GFP protein below that seen with the empty vector, without decreasing *GFP* mRNA levels (Figure 4, A and B, compare lanes 1 and 3). Neither deletion nor overexpression of Khd1 affects protein or mRNA levels from constructs lacking the *FLO11* repetitive element (Figure 4, A and B, lanes 5–8, and Figure S4). In addition to repressing transcription of *FLO11* by regulating *ASH1* expression, Khd1 represses translation through its interaction with repeated sequences in *FLO11* mRNA.

Translational repression of the fusion construct is consistent with the post-transcriptional repression of Flo11 protein expression by Khd1. Although Khd1 does not appear to regulate endogenous *FLO11* mRNA levels independent of *ASH1* (Figure 2), mRNA levels from the construct with the *FLO11* repeats fused to *GFP* increase in the *khd1*Δ mutant (Figure 4B). The fusion transcript may be subject to different regulation than *FLO11* mRNA independent of Khd1. Alternatively, low levels of *FLO11* mRNA in the *ash1*Δ/*ash1*Δ mutant may preclude detection of small changes in stability. To test *FLO11* mRNA stability, we used the *ADH* promoter to transcribe full-length *FLO11* mRNA and measured its steady-state levels, similar to our measurement of mRNA from the fusion construct. In the *khd1*Δ mutant, *FLO11* mRNA levels from this construct are 63% of those in wild type. Changes in mRNA stability alone do not explain the differences between mRNA and protein levels for either the fusion construct or endogenous *FLO11* in the absence of Khd1. Therefore, translational repression through the repeats is the predominant post-transcriptional regulation of *FLO11* mRNA by Khd1.

Khd1 regulates Flo11 asymmetry: Flo11 protein expression determines daughter cell fate during filamentous growth. To determine whether the transcriptional and translational regulation by Khd1 affects Flo11 expression between mother and daughter cells, we scored Flo11 expression patterns using the *FLO11::HA* allele and fluorescence microscopy. The four possible expression patterns between mother and daughter cells were each observed (Figure 5A). Mother cells that express Flo11 can give rise to daughter cells that also express the protein, or those that switch Flo11 expression off. Reciprocally, mother cells that do not express Flo11 can produce daughter cells that similarly do not express the protein, or those that switch Flo11 expression on. We

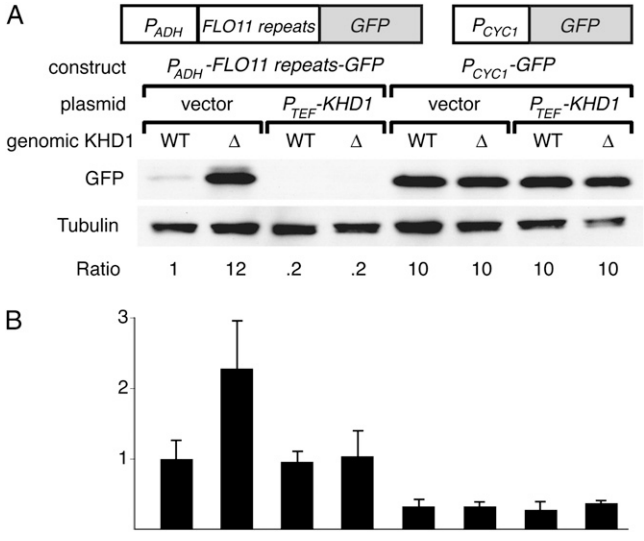

FIGURE 4.—Khd1 represses translation through the *FLO11* repeats. (A) Western blot analysis of GFP protein levels from constructs expressing GFP alone, or GFP fused to the *FLO11* repetitive sequences. P_{TEF}–*KHD1* is an overexpression construct. The only visible band detected from wild type, and the predominant band from *khd1*Δ, migrate at the same molecular weight as GFP alone, suggesting that translation initiated at the GFP start codon. The higher migrating band from *khd1*Δ may result from low levels of translation initiation inside the repetitive element that become visible after derepression. (B) GFP mRNA levels normalized to *TUB1* mRNA levels for the strains shown in A. Values are average of four independent experiments. Error reported as standard deviation.

calculated probabilities for daughter cell Flo11 expression given the Flo11 expression of the mother cell based on the frequencies of these expression patterns

Repression by Khd1 reduces the frequency of Flo11 expression in daughter cells. Compared to wild-type daughter cells, *khd1*Δ*/khd1*Δ daughter cells are more likely to express Flo11 protein whether or not it is expressed in the mother (Figure 5B). These increases result from the loss of the combined transcriptional and translational repression of *FLO11* by Khd1. More *khd1*Δ*/khd1*Δ *ash1*Δ*/ash1*Δ daughter cells than *ash1*Δ*/ash1*Δ daughter cells also express Flo11 protein whether or not it is expressed in the mother (Figure 5B). These increases result solely from the loss of translational repression by Khd1, since the deletion of *ASH1* inactivates the transcriptional regulation. Although the loss of Khd1-mediated translational repression of *FLO11* mRNA increases the expression of Flo11 protein in daughter cells, maximal induction of Flo11 expression in daughter cells, seen in the *khd1*Δ*/khd1*Δ mutant, requires the dual relief of both the transcriptional and translational repression of *FLO11* by Khd1.

Khd1 binds many mRNAs that encode cell wall proteins: Khd1 binds a number of mRNAs encoding cell wall proteins in addition to *FLO11* mRNA. Fifty-four of the Khd1 target mRNAs we identify using CLIP (Table S4) encode proteins that play a role in cell wall function, nearly half of the 114 genes with this annotation ($p = 5.85 \times 10^{-15}$) (Beissbarth and Speed 2004). Similar to *FLO11* mRNA, many of the Khd1 targets that encode cell surface proteins contain repeated sequences. When target genes are sorted by the number of sequences that map to their binding sites, 9 of the top 10—*FLO11, SED1, YIL169C, AGA1, SCW10, MSB2, RPO21, CRH1,* and *YNL190W*—contain repeats (reported in Verstrepen *et al.* 2005 or determined by visual inspection) and 8 of these 9 encode cell surface proteins, with the lone exception being *RPO21*. With the exception of *CRH1* mRNA, Khd1 binds these nine transcripts through their repetitive elements (Figure S5 and Figure 3B), implying that Khd1 frequently binds repeated sequences. Khd1 appears to have a bias for messages with repeated sequences as it binds mRNAs transcribed from 32 of the 44 *S. cerevisiae* genes previously reported to contain intragenic repeats (Verstrepen *et al.* 2005).

However, the presence of repeats is not the only determinant of Khd1 binding. First, not all mRNAs bound by Khd1 have repeated sequences. Second, in some cases where Khd1 binds to messages with repeated sequences, the binding is not in the region of repeats (Figure S3, *CRH1*). Third, Khd1 does not bind all mRNAs that contain repeated sequences.

To understand the determinants of recognition by Khd1, we analyzed the sequences within its binding sites. MEME analysis (Bailey and Elkan 1994) produces a degenerate octamer motif (Figure 6) that occurs in 12% of the Khd1 binding sites. This result is consistent with the CNN repeats found to mediate Khd1 binding in a previous study (Hasegawa *et al.* 2008). Examination of our motif reveals additional features that may contribute to the interaction between Khd1 and its target RNAs. The repeating CA pattern is similar to the one found in RNAs recognized by the mammalian RNA-binding protein Nova (Buckanovich and Darnell 1997; Jensen *et al.* 2000; Ule *et al.* 2003; Licatalosi *et al.* 2008). Khd1 and Nova both contain three K-homology RNA-binding domains (Currie and Brown 1999; Buckanovich *et al.* 1993), and structural studies indicate that the third KH domain in Nova makes specific contacts with the internal CA in a YCAY (where Y indicates a pyrimidine, U or C) tetramer (Lewis *et al.* 2000). CA is the most enriched dinucleotide (1.8-fold relative to background) in the Khd1 binding sites. Two of the four tetranucleotides with the highest enrichments relative to background—CAAC, CUCC, CAUC, and CUAC are enriched 3.3-, 3.0-, 2.9-, and 2.6-fold, respectively—contain CA in the first and second position, but not internally as in the YCAY motif. All four contain C in the first and last position. This analysis identifies new possible determinants of recognition by Khd1, but despite our high-resolution detection of *in vivo* binding sites, we do not find a motif to explain the specificity of Khd1 for all of its RNA targets.

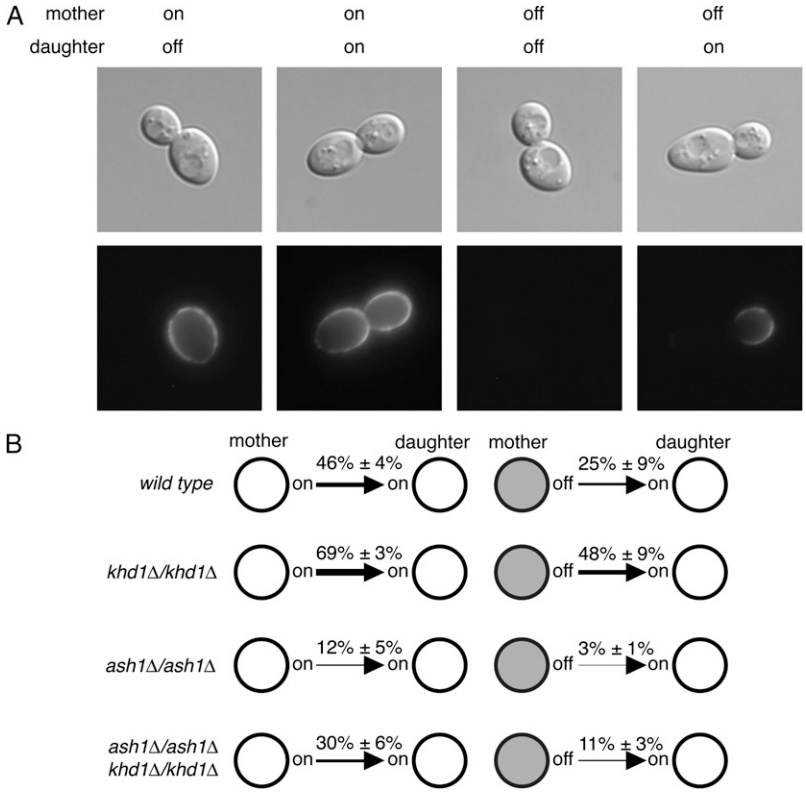

FIGURE 5.—Khd1 regulates mother–daughter Flo11 expression. Fluorescence microscopy was used to visualize Flo11 protein expression from the *FLO11::HA* allele. (A) Flo11 expression patterns in mother–daughter pairs. (B) Khd1 affects the frequency at which daughter cells express Flo11 protein. The chance that a mother cell gives rise to a daughter cell expressing Flo11 protein increases when *KHD1* is deleted, independent of *ASH1* and whether or not the mother cell expresses Flo11 protein. The frequency of a daughter cell expressing Flo11 protein being produced from a mother cell that expresses Flo11 protein was determined by dividing the number of these mother–daughter pairs by the total number of pairs in which the mother expresses Flo11 protein. The frequency of a daughter cell expressing Flo11 protein being produced from a mother cell that does not express Flo11 protein was determined by dividing the number of these mother–daughter pairs by the total number of pairs in which the mother does not express Flo11. Two hundred and fifty mother-daughter pairs were analyzed per genotype in each of nine separate trials. Error reported as standard deviation.

DISCUSSION

Our genetic and biochemical studies show that Khd1 acts post-transcriptionally on two mRNAs to repress *FLO11* expression and filamentation. Previous studies showed that *ASH1* activates *FLO11* expression (PAN and HEITMAN 2000) and filamentous growth (CHANDARLAPATY and ERREDE 1998) and that Khd1 represses translation of *ASH1* mRNA in the context of mating-type switching (IRIE *et al.* 2002; PAQUIN *et al.* 2007; HASEGAWA *et al.* 2008). Our results demonstrate that Khd1 represses *FLO11* expression both through its regulation of *ASH1* and by directly inhibiting translation of *FLO11* mRNA through repetitive sequences in the open reading frame. This dual inhibition places Khd1 at the head of a feed-forward loop regulating *FLO11* (Figure 7) and raises the question of why cells employ this regulatory architecture.

The answer may reside in the biology of *FLO11*, whose function is required to switch from the yeast form to the filamentous form (LAMBRECHTS *et al.* 1996; LO and DRANGINIS 1998; HALME *et al.* 2004). In the first cell cycle under conditions of nitrogen starvation, over 90% of yeast-form cells produce a filamentous bud (AHN *et al.* 1999). The immediate relief of Khd1-mediated translational repression on an existing pool of *FLO11* mRNA would allow for the rapid production of Flo11 protein in the first daughter cell even if the mother cell did not express the protein during yeast-form growth. This effect is seen in comparing Flo11 protein expression between *ash1*Δ*/ash1*Δ and *khd1*Δ*/khd1*Δ *ash1*Δ*/ash1*Δ. More *khd1*Δ*/khd1*Δ *ash1*Δ*/ash1*Δ cells express Flo11 protein than *ash1*Δ*/ash1*Δ cells (Table 1), resulting from the higher likelihood that a daughter cell expresses Flo11 protein whether or not it is expressed in the mother cell (Figure 5B). Given that there is not a concomitant increase in *FLO11* mRNA levels (Figure 2), this change represents increased translation of *FLO11* mRNA upon the loss of Khd1-mediated repression. The rapid inductive response leading to filamentation in the daughter suggests that repression by Khd1 may be quickly relieved under conditions of nitrogen starvation.

A filamentous cell expressing Flo11 protein can divide to produce a yeast-form cell that does not express Flo11 protein (HALME *et al.* 2004). Such a rapid transition may require inhibition of both transcription and translation of *FLO11* mRNA. This dual control would repress preexisting *FLO11* mRNA from the mother and prevent the daughter from transcribing new *FLO11* mRNA. Khd1 can execute both of these functions to produce asymmetric Flo11 protein expression. Since Flo11 protein is required in the daughter cell to maintain filamentous growth, the increase in Flo11 protein expression when repression by Khd1 is lost in the *khd1*Δ*/khd1*Δ mutant (Table 1, Figure 5C) likely explains its hyperfilamentation phenotype (Figure 1A).

This model for asymmetric *FLO11* expression and developmental switching posits differential Khd1 activity between cells. This heterogeneity would explain a surprising aspect of the changes in Flo11 protein expression between the *ash1*Δ*/ash1*Δ and *khd1*Δ*/khd1*Δ

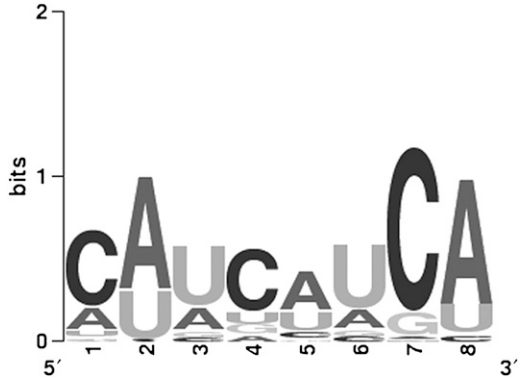

Figure 6.—Motif recognized by Khd1. MEME result (Bailey and Elkan 1994) from the sequences within the binding sites identified by CLIP.

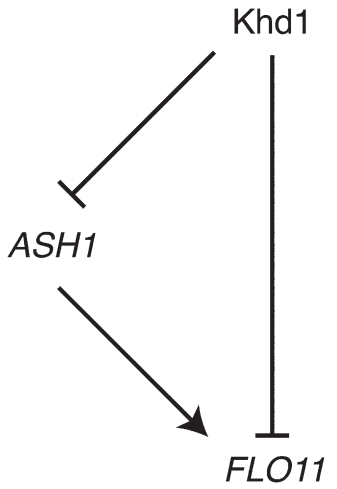

Figure 7.—Feed-forward regulation of *FLO11* by Khd1. Khd1 regulates transcription of *FLO11* through its repression of *ASH1* mRNA and directly represses translation by binding repeated sequences in the open reading frame of *FLO11* mRNA.

*ash1*Δ*/ash1*Δ mutants. In the absence of *ASH1*, the loss of Khd1 enables a higher percentage of cells to express Flo11 protein, but not more of it (Table 1). Individual cells can therefore express Flo11 protein at the same level whether or not they can express Khd1. Because *ASH1* is deleted, deletion of *KHD1* relieves translational repression on *FLO11* mRNA, but does not affect *FLO11* transcription (Figure 7). If Khd1 repressed translation of *FLO11* mRNA uniformly across all cells, its absence in *khd1*Δ*/khd1*Δ *ash1*Δ*/ash1*Δ cells would result in increased levels of Flo11 protein. Instead, it appears that some cells containing Khd1 fail to repress translation of *FLO11* mRNA, and deletion of *KHD1* simply expands this population. Phosphorylation of Khd1 by Yck1 regulates its repression of *ASH1* mRNA during mating-type switching (Paquin *et al.* 2007). Although deletion of *YCK1* does not affect filamentous growth (data not shown), post-translational modifications may regulate Khd1 to generate heterogeneous activity and enable the rapid changes in *FLO11* expression that underlie asymmetry during filamentous growth.

The asymmetry that arises when a yeast-form mother cell produces a filamentous daughter cell has similarities to the asymmetry of mothers and daughters with respect to mating-type switching. In both morphogenetic events, the mother and daughter have different developmental outcomes dependent on asymmetric gene expression. The two processes also have some differences. One striking difference is that Ash1 activates filamentation but represses mating-type switching, which could reflect the different potentials of the mother and daughter cells between the two processes. The asymmetric expression of *ASH1* allows the mother to switch mating type, but prevents the daughter from doing so (Strathern and Herskowitz 1979; Chartrand *et al.* 2002; Paquin and Chartrand 2008). However, an elliptical yeast-form mother cell already encased in a cell wall of defined structure does not elongate. Instead it is the daughter cell that must express Flo11 protein to develop into a filamentous cell.

The developmental potential of the mother cell is constrained because filamentous growth requires a different program for construction of the cell wall. In this context it may be significant that Khd1 binds 54 mRNAs that encode proteins annotated to function in this macromolecular structure. Post-transcriptional regulation of these genes by Khd1 could provide a unifying mechanism for constructing this organelle. One mechanism for coordinating translational control of these messages would be to have a signature binding site in the mRNAs dedicated to this function. Although we observe a motif consistent with a previous report that used other methods to identify Khd1 binding sites (Hasegawa *et al.* 2008), we do not identify a sequence that comprehensively explains recognition by Khd1. These data suggest that although the motif we identify contributes to target recognition by Khd1, there must be additional recognition determinants.

Our studies identify a new biological role for Khd1. Its bipartite repression of *FLO11* provides dynamic regulation that controls the expression of a cell fate determinant in the daughter cell. Given the prevalence of sequences derived from *FLO11* in the CLIP experiment, this likely represents a major function for Khd1. Khd1 binds a number of transcripts that encode cell wall proteins through repetitive sequences in addition to *FLO11* mRNA, and Khd1 may regulate the synthesis of many proteins that play a role in this structure. The documented expansion and contraction of the repeats bound by Khd1 (Verstrepen *et al.* 2005) would generate target sequences of diverse lengths that could be bound differentially, and as a consequence produce altered levels of these cell surface proteins. These changes could have important consequences for the structure and function of the yeast cell wall.

We thank the members of the laboratories of G.R.F. and D.K.G. for discussions; A. Mele and R. Darnell for advice and technical support with CLIP; A. Rolfe for assistance with computational methods; B. Chin for critical reading of the manuscript. This work was supported by National Institutes of Health Grants GM040266, GM069676, and GM035010 and the Abraham Siegel Fellowship and National Science Foundation Graduate Research Fellowship to J.J.W. G.R.F is an American Cancer Society Professor.

LITERATURE CITED

Ahn, S. H., A. Acurio and S. J. Kron, 1999 Regulation of G2/M progression by the STE mitogen-activated protein kinase pathway in budding yeast filamentous growth. Mol. Biol. Cell **10:** 3301–3316.

Bailey, T. L., and C. Elkan, 1994 Fitting a mixture model by expectation maximization to discover motifs in biopolymers. Proc. Int. Conf. Intell. Syst. Mol. Biol. **2:** 28–36.

Bailey, T. L., and M. Gribskov, 1998 Combining evidence using p-values: application to sequence homology searches. Bioinformatics **14:** 48–54.

Beissbarth, T., and T. P. Speed, 2004 GOstat: find statistically overrepresented Gene Ontologies within a group of genes. Bioinformatics **20:** 1464–1465.

Bobola, N., R. P. Jansen, T. H. Shin and K. Nasmyth, 1996 Asymmetric accumulation of Ash1p in postanaphase nuclei depends on a myosin and restricts yeast mating-type switching to mother cells. Cell **84:** 699–709.

Buckanovich, R. J., and R. B. Darnell, 1997 The neuronal RNA binding protein Nova-1 recognizes specific RNA targets in vitro and in vivo. Mol. Cell. Biol. **17:** 3194–3201.

Buckanovich, R. J., J. B. Posner and R. B. Darnell, 1993 Nova, the paraneoplastic Ri antigen, is homologous to an RNA-binding protein and is specifically expressed in the developing motor system. Neuron **11:** 657–672.

Bumgarner, S. L., R. D. Dowell, P. Grisafi, D. K. Gifford and G. R. Fink, 2009 Toggle involving cis-interfering noncoding RNAs controls variegated gene expression in yeast. Proc. Natl. Acad. Sci. USA **106:** 18321–18326.

Chandarlapaty, S., and B. Errede, 1998 Ash1, a daughter cell-specific protein, is required for pseudohyphal growth of *Saccharomyces cerevisiae*. Mol. Cell. Biol. **18:** 2884–2891.

Chartrand, P., X. H. Meng, S. Huttelmaier, D. Donato and R. H. Singer, 2002 Asymmetric sorting of "Ash1p" in yeast results from inhibition of translation by localization elements in the mRNA. Mol. Cell **10:** 1319–1330.

Currie, J. R., and W. T. Brown, 1999 KH domain-containing proteins of yeast: absence of a fragile X gene homologue. Am. J. Med. Genet. **84:** 272–276.

Danford, T. W., R. D. Dowell, S. Agarwala, P. Grisafi, G. R. Fink *et al.*, 2010 Discovering regulatory overlapping RNA transcripts. Fourteenth International Conference on Research in Computational Molecular Biology**,** Lisbon, Portugal.

Dowell, R. D., O. Ryan, A. Jansen, D. Cheung, S. Agarwala *et al.*, 2010 Genotype to phenotype: a complex problem. Science **328:** 469.

Gerber, A. P., D. Herschlag and P. O. Brown, 2004 Extensive association of functionally and cytotopically related mRNAs with Puf family RNA-binding proteins in yeast. PLoS Biol. **2:** E79.

Ghaemmaghami, S., W. K. Huh, K. Bower, R. W. Howson, A. Belle *et al.*, 2003 Global analysis of protein expression in yeast. Nature **425:** 737–741.

Gimeno, C. J., P. O. Ljungdahl, C. A. Styles and G. R. Fink, 1992 Unipolar cell divisions in the yeast *S. cerevisiae* lead to filamentous growth: regulation by starvation and RAS. Cell **68:** 1077–1090.

Guo, B., C. A. Styles, Q. Feng and G. R. Fink, 2000 A Saccharomyces gene family involved in invasive growth, cell-cell adhesion, and mating. Proc. Natl. Acad. Sci. USA **97:** 12158–12163.

Guthrie, C., and G. R. Fink, 1991 *Guide to Yeast Genetics and Molecular Biology*. Academic Press, San Diego.

Halme, A., S. Bumgarner, C. Styles and G. R. Fink, 2004 Genetic and epigenetic regulation of the FLO gene family generates cell-surface variation in yeast. Cell **116:** 405–415.

Hasegawa, Y., K. Irie and A. P. Gerber, 2008 Distinct roles for Khd1p in the localization and expression of bud-localized mRNAs in yeast. RNA **14:** 2333–2347.

Hogan, D. J., D. P. Riordan, A. P. Gerber, D. Herschlag and P. O. Brown, 2008 Diverse RNA-binding proteins interact with functionally related sets of RNAs, suggesting an extensive regulatory system. PLoS Biol. **6:** e255.

Horvitz, H. R., and I. Herskowitz, 1992 Mechanisms of asymmetric cell division: two Bs or not two Bs, that is the question. Cell **68:** 237–255.

Irie, K., T. Tadauchi, P. A. Takizawa, R. D. Vale, K. Matsumoto *et al.*, 2002 The Khd1 protein, which has three KH RNA-binding motifs, is required for proper localization of ASH1 mRNA in yeast. EMBO J. **21:** 1158–1167.

Janke, C., M. M. Magiera, N. Rathfelder, C. Taxis, S. Reber *et al.*, 2004 A versatile toolbox for PCR-based tagging of yeast genes: new fluorescent proteins, more markers and promoter substitution cassettes. Yeast **21:** 947–962.

Jensen, K. B., K. Musunuru, H. A. Lewis, S. K. Burley and R. B. Darnell, 2000 The tetranucleotide UCAY directs the specific recognition of RNA by the Nova K-homology 3 domain. Proc. Natl. Acad. Sci. USA **97:** 5740–5745.

Keene, J. D., 2007 RNA regulons: coordination of post-transcriptional events. Nat. Rev. Genet. **8:** 533–543.

Lambrechts, M. G., F. F. Bauer, J. Marmur and I. S. Pretorius, 1996 Muc1, a mucin-like protein that is regulated by Mss10, is critical for pseudohyphal differentiation in yeast. Proc. Natl. Acad. Sci. USA **93:** 8419–8424.

Lewis, H. A., K. Musunuru, K. B. Jensen, C. Edo, H. Chen *et al.*, 2000 Sequence-specific RNA binding by a Nova KH domain: implications for paraneoplastic disease and the fragile X syndrome. Cell **100:** 323–332.

Licatalosi, D. D., A. Mele, J. J. Fak, J. Ule, M. Kayikci *et al.*, 2008 HITS-CLIP yields genome-wide insights into brain alternative RNA processing. Nature **456:** 464–469.

Liu, H., C. A. Styles and G. R. Fink, 1996 *Saccharomyces cerevisiae* S288C has a mutation in FLO8, a gene required for filamentous growth. Genetics **144:** 967–978.

Lo, W. S., and A. M. Dranginis, 1998 The cell surface flocculin Flo11 is required for pseudohyphae formation and invasion by *Saccharomyces cerevisiae*. Mol. Biol. Cell **9:** 161–171.

Long, R. M., R. H. Singer, X. Meng, I. Gonzalez, K. Nasmyth *et al.*, 1997 Mating type switching in yeast controlled by asymmetric localization of ASH1 mRNA. Science **277:** 383–387.

Macara, I. G., and S. Mili, 2008 Polarity and differential inheritance: universal attributes of life? Cell **135:** 801–812.

Mumberg, D., R. Muller and M. Funk, 1995 Yeast vectors for the controlled expression of heterologous proteins in different genetic backgrounds. Gene **156:** 119–122.

Pan, X., and J. Heitman, 2000 Sok2 regulates yeast pseudohyphal differentiation via a transcription factor cascade that regulates cell-cell adhesion. Mol. Cell. Biol. **20:** 8364–8372.

Paquin, N., and P. Chartrand, 2008 Local regulation of mRNA translation: new insights from the bud. Trends Cell Biol. **18:** 105–111.

Paquin, N., M. Menade, G. Poirier, D. Donato, E. Drouet *et al.*, 2007 Local activation of yeast ASH1 mRNA translation through phosphorylation of Khd1p by the casein kinase Yck1p. Mol. Cell **26:** 795–809.

Rabani, M., M. Kertesz and E. Segal, 2008 Computational prediction of RNA structural motifs involved in posttranscriptional regulatory processes. Proc. Natl. Acad. Sci. USA **105:** 14885–14890.

Sanford, J. R., X. Wang, M. Mort, N. Vanduyn, D. N. Cooper *et al.*, 2009 Splicing factor SFRS1 recognizes a functionally diverse landscape of RNA transcripts. Genome Res. **19:** 381–394.

Sil, A., and I. Herskowitz, 1996 Identification of asymmetrically localized determinant, Ash1p, required for lineage-specific transcription of the yeast HO gene. Cell **84:** 711–722.

Strathern, J. N., and I. Herskowitz, 1979 Asymmetry and directionality in production of new cell types during clonal growth: the switching pattern of homothallic yeast. Cell **17:** 371–381.

Ule, J., K. B. Jensen, M. Ruggiu, A. Mele, A. Ule *et al.*, 2003 CLIP identifies Nova-regulated RNA networks in the brain. Science **302:** 1212–1215.

Ule, J., K. Jensen, A. Mele and R. B. Darnell, 2005 CLIP: a method for identifying protein-RNA interaction sites in living cells. Methods **37:** 376–386.

Verstrepen, K. J., A. Jansen, F. Lewitter and G. R. Fink, 2005 Intragenic tandem repeats generate functional variability. Nat. Genet. **37:** 986–990.

Winzeler, E. A., D. D. Shoemaker, A. Astromoff, H. Liang, K. Anderson *et al.*, 1999 Functional characterization of the *S. cerevisiae* genome by gene deletion and parallel analysis. Science **285:** 901–906.

Yao, Z., Z. Weinberg and W. L. Ruzzo, 2006 CMfinder: a covariance model based RNA motif finding algorithm. Bioinformatics **22:** 445–452.

Yeo, G. W., N. G. Coufal, T. Y. Liang, G. E. Peng, X. D. Fu *et al.*, 2009 An RNA code for the FOX2 splicing regulator revealed by mapping RNA-protein interactions in stem cells. Nat. Struct. Mol. Biol. **16:** 130–137.

Communicating editor: M. D. Rose

GENETICS

Supporting Information
http://www.genetics.org/cgi/content/full/genetics.109.113944/DC1

Feed-Forward Regulation of a Cell Fate Determinant by an RNA-Binding Protein Generates Asymmetry in Yeast

Joshua J. Wolf, Robin D. Dowell, Shaun Mahony, Michal Rabani, David K. Gifford and Gerald R. Fink

DOI: 10.1534/genetics.109.113944

FILE S1

Supporting Methods

Cross-linking Immunoprecipitation: 1 L of cells containing the *KHD1-TAP* allele were harvested at OD 2.5, washed twice with water and resuspended in 10X pellet volume. UV crosslinking was performed by irradiating shallow layers of this suspension three times at 400 mJ/cm^2. Cells were washed in calmodulin binding buffer (CBB) with .1% NP-40 (RIGAUT *et al.* 1999) and protease inhibitors (leupeptin, pepstatin, PMSF), resuspended in 10 mL and separated and into FastPrep tubes. 600 micron glass beads were added to ~1/3 volume and lysis performed three times, 45 seconds at maximum speed in a FastPrep 3000.

The lysate was collected by puncturing the bottom of the tube and spinning the sample into a 15 mL tube. Samples were spun at 3,000 rpm for 5 minutes and the supernatant was collected. The pellet was resuspended in 5 mL CBB with .1% NP-40 and protease inhibitors, spun again at 3,000 rpm for 5 minutes, and the supernatant collected. This process was repeated one more time. RNAse A (USB 70194Y) was added to the pooled supernatants at a dilution of 1:50,000 or 1:1,000 and incubated at 37° Celsius for 10 minutes. The sample was split into microcentrifuge tubes and spun at 9,500 rpm for 5 minutes. The supernatant was transferred to fresh tubes and spun at 12,000 rpm for 5 minutes. The supernatant was used for immunoprecipitation.

300 μL calmodulin-agarose beads (GE Healthcare 17-0529-01) were equilibrated for ten minutes in CBB with .1% NP-40 three times. The equilibrated beads were added to the supernatant and incubated for 2 hours at 4° Celsius on a rocking platform. The beads were collected through a column and washed twice in 5 mL CBB with .1% NP-40 and twice in 5 mL CBB with .02% NP-40. Protein was incubated in 3 mL calmodulin elution buffer (CEB) (RIGAUT *et al.* 1999) for 45 minutes at 4° Celsius on a rocking platform and then collected in a 15 mL tube. The beads were twice washed with 1 mL CEB which was pooled with the initial eluate.

800 μL Dynalbeads (Invitrogen 112-010) were equilibrated in CEB three times for ten minutes, added to the eluate, and incubated for 1 hour at 4° Celsius on a rocking platform. The beads were collected using a magnet and transferred to a microcentrifuge tube. They were washed with Nelson stringent buffer (5 mM Tris, pH 7.5, 5 mM EDTA, 2.5 mM EGTA, 1% Triton X-100, 1% Na-DOC, 0.1% SDS, 120 mM NaCl, 25 mM KCl) followed by Nelson high salt buffer (15 mM Tris, pH 7.5, 5 mM EDTA, 2.5 mM EGTA, 1% Triton X-100, 1% Na-DOC, 0.1% SDS, 1 M NaCl) for 10 minutes each at 4° Celsius on a rocking platform and transferred to a new tube where they were washed twice in Nelson low salt buffer (15 mM Tris, pH 7.5, 5 mM EDTA).

After this immunoprecipitation, the CLIP protocol was followed as previously described to obtain DNA molecules for sequencing (ULE *et al.* 2005), with the exception of the primers used for cDNA amplification as noted in the main text.

LITERATURE CITED

RIGAUT, G., A. SHEVCHENKO, B. RUTZ, M. WILM, M. MANN *et al.*, 1999 A generic protein purification method for protein complex characterization and proteome exploration. Nat Biotechnol **17:** 1030-1032.

ULE, J., K. JENSEN, A. MELE and R. B. DARNELL, 2005 CLIP: a method for identifying protein-RNA interaction sites in living cells. Methods **37:** 376-386.

FILE S2

Supporting Results

CLIP Specificity: Multiple control experiments were conducted to ensure that CLIP specifically identified *in vivo* RNA targets of Khd1. As part of this analysis, Khd1-RNA complex formation was visualized by end labeling RNAs following immunoprecipitation of Khd1-TAP and treatment with RNAse A as previously described (ULE *et al.* 2005). Non-specific RNA contaminants migrate at a much lower molecular weight than protein-RNA complexes, and can be separated using SDS-PAGE. Additionally, transfer to nitrocellulose membrane retains the protein-RNA complexes, but not free RNA (SANFORD *et al.* 2008; ULE *et al.* 2003). Khd1-RNA complexes were then visualized using autoradiography.

Khd1-RNA complex formation requires UV crosslinking (Figure S2) as has been previously demonstrated using mammalian RNA-binding proteins (SANFORD *et al.* 2008; ULE *et al.* 2003). Khd1-TAP has a predicted molecular weight of approximately 63 kilodaltons (kDa), but Western blot analysis shows the protein migrates at slightly less than 75 kDa during SDS-PAGE (data not shown). When a high concentration of RNAse A is used, Khd1-RNA complexes migrate slightly higher than 75 kDa (Figure S2). With lower RNAse A concentrations, longer RNA molecules are maintained leading to an increase in the molecular weight of the complexes (Figure S2).

Immunoprecipitation of Khd1-TAP from un-crosslinked cells was used to determine whether pure samples of Khd1 were obtained. Mass spectrometry of the band at about 75 kDa revealed no major protein species co-migrating with Khd1-TAP (data not shown), suggesting the signal on the autoradiogram derives specifically from Khd1-RNA complexes.

Immunoprecipitation of other RNA-binding proteins following crosslinking resulted in the formation of protein-RNA complexes of an expected size based on the molecular weight of the protein, but no complexes were seen when proteins without RNA-binding domains were used (data not shown).

Based on the above results, we conclude the sequences we obtained derive specifically from interactions between Khd1 and its endogenous RNA targets.

LITERATURE CITED

SANFORD, J. R., P. COUTINHO, J. A. HACKETT, X. WANG, W. RANAHAN *et al.*, 2008 Identification of nuclear and cytoplasmic mRNA targets for the shuttling protein SF2/ASF. PLoS One **3:** e3369.

ULE, J., K. JENSEN, A. MELE and R. B. DARNELL, 2005 CLIP: a method for identifying protein-RNA interaction sites in living cells. Methods **37:** 376-386.

ULE, J., K. B. JENSEN, M. RUGGIU, A. MELE, A. ULE *et al.*, 2003 CLIP identifies Nova-regulated RNA networks in the brain. Science **302:** 1212-1215.

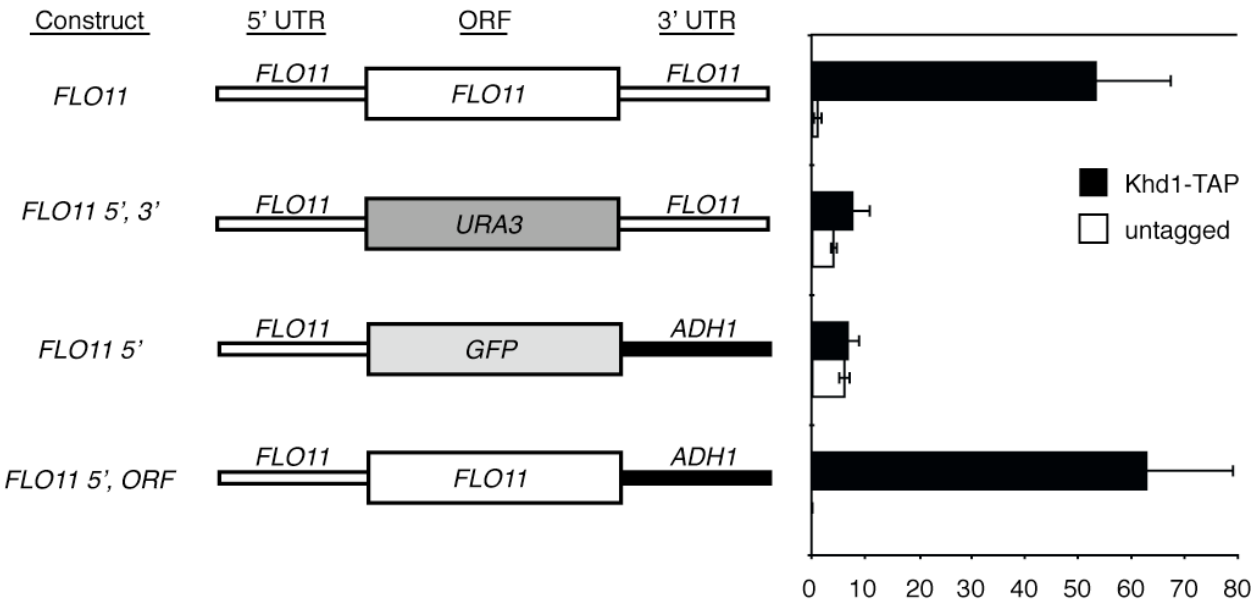

FIGURE S1.—Khd1 Interaction with *FLO11* mRNA requires the ORF. Enrichment following immunoprecipitation from cells expressing Khd1-TAP or untagged Khd1 calculated as in Figure 3. The *FLO11 5', 3'* construct contains a complete replacement of the *FLO11* ORF with *URA3*. The *FLO11* 5' and 3' UTRs remain intact in this construct. The *FLO11 5'* construct retains the *FLO11* 5' UTR but replaces everything downstream of the start codon with *GFP* followed by the *ADH1* 3' UTR. The *FLO11 5', ORF* construct maintains the *FLO11* 5' UTR and ORF but substitutes the *ADH1* 3' UTR for the *FLO11* 3' UTR. Neither *FLO11* UTR is sufficient for the interaction with Khd1; immunoprecipitation of Khd1-TAP only enriches transcripts containing the *FLO11* ORF.

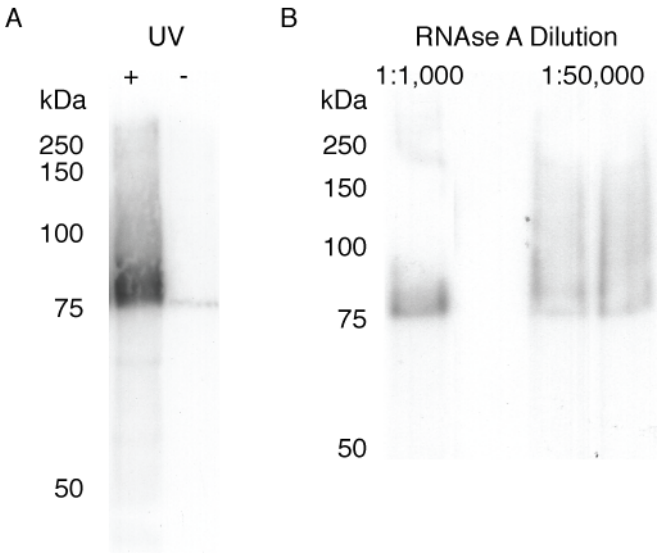

FIGURE S2.— CLIP identifies RNA targets of Khd1. Following immunoprecipitation of Khd1-TAP, protein RNA complexes were labeled as previously described (ULE et al. 2005), separated by size using SDS-PAGE, and visualized using autoradiography. (A) Khd1-RNA complex formation is dependent on UV crosslinking. (B) Increased digestion with RNAse A increases complex mobility. A band from the sample with the 1:50,000 RNAse A dilution was isolated for sequencing as previously described (ULE et al. 2005).

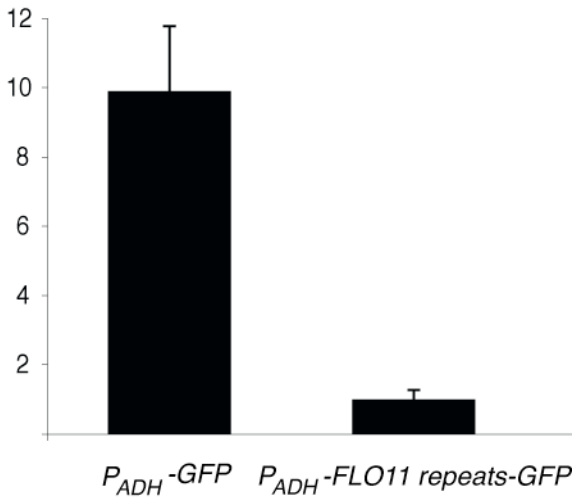

FIGURE S3.—Fusion to the *FLO11* repeats decreases *GFP* mRNA levels. *GFP* mRNA normalized to *TUB1* mRNA. Constructs diagrammed in Figure 4. Values are average of four independent experiments. Error reported as standard deviation.

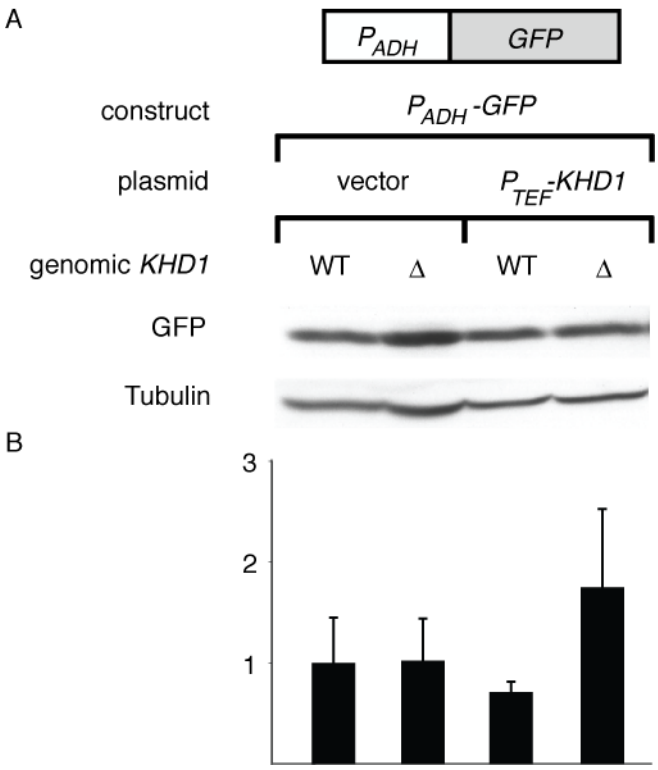

FIGURE S4.—*KHD1* does not affect expression from the *ADH* promoter. (A) Western blot analysis of P_{ADH} – *GFP* reporter construct. (B) *GFP* mRNA normalized to *TUB1* mRNA for the strains shown in (A). Values are average of four independent experiments. Error reported as standard deviation.

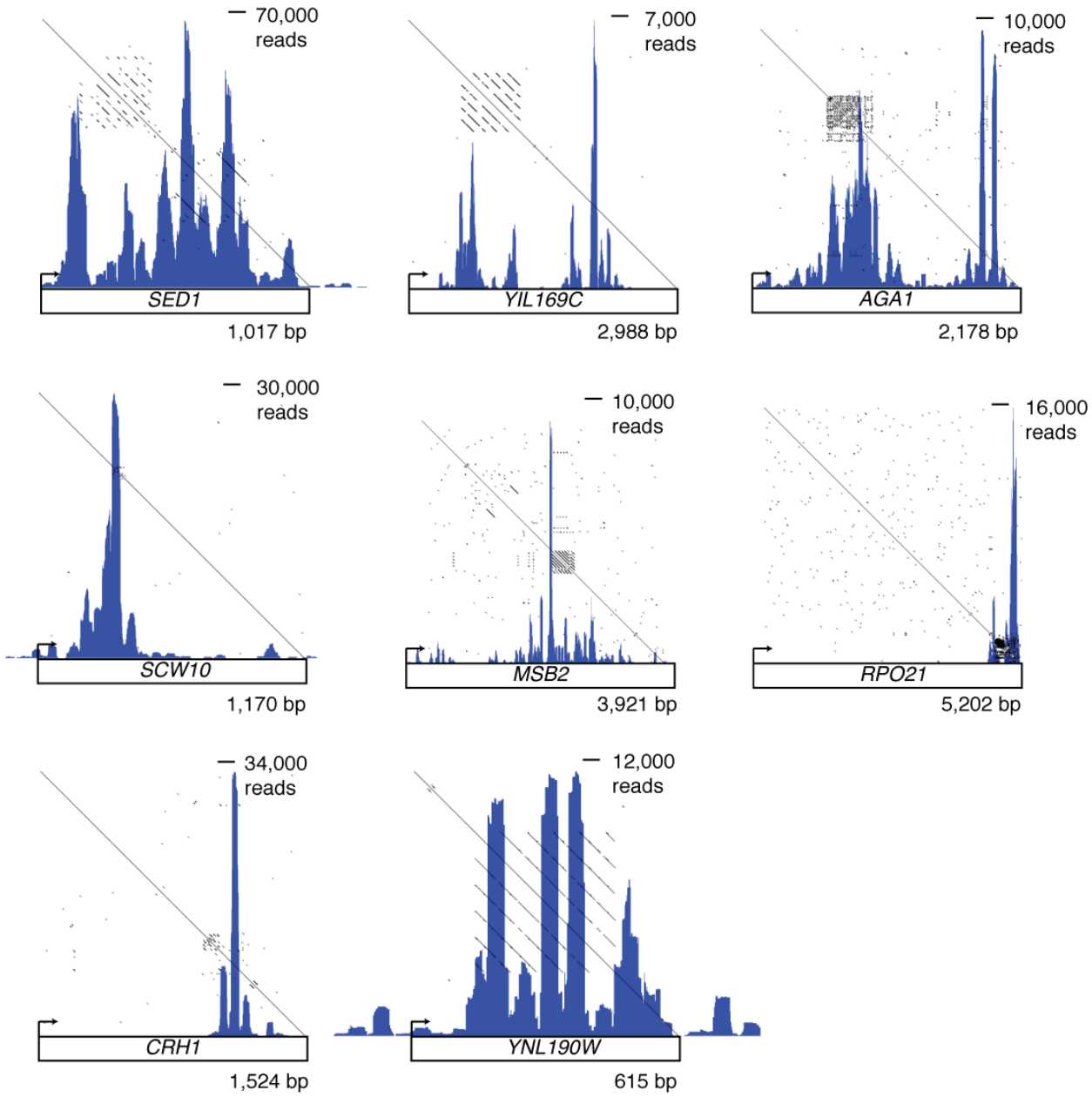

FIGURE S5.—Top Khd1 targets contain repetitive sequences. Nine of the top ten targets identified by CLIP contain internal repeats (*FLO11* depicted in Figure 3B). Histogram of read density from CLIP experiment overlaid on a dot plot highlighting the repetitive region of each ORF. For each ORF, histogram scale shown at top right, ORF length shown at bottom right. See Figure 4 for dot plot specifications.

TABLE S1

Yeast strains and plasmids used in this study

Strain	Genotype	Source
JW971	*MATa/α his3::hisG/his3::hisG ura3-52/ura3-52*	This study
JW1064	*MATa/α his3::hisG/his3::hisG ura3-52/ura3-52 khd1::kanMX4/khd1::kanMX4*	This study
JW1066	*MATa/α his3::hisG/his3::hisG ura3-52/ura3-52 ash1::kanMX4/ash1::kanMX4*	This study
JW1068	*MATa/α his3::hisG/his3::hisG ura3-52/ura3-52 flo11::kanMX4/flo11::kanMX4*	This study
JW1033	*MATa/α his3::hisG/his3::hisG ura3-52/ura3-52 ash1::kanMX4/ash1::kanMX4 khd1::kanMX4/khd1::kanMX4*	This study
JW1027	*MATa/α his3::hisG/his3::hisG ura3-52/ura3-52 flo11::kanMX4/flo11::kanMX4 khd1::kanMX4/khd1::kanMX4*	This study
JW928	*MATα his3::hisG ura3-52*	This study
JW994	*MATα his3::hisG ura3-52 khd1::kanMX4*	This study
JW1052	*MATα his3::hisG ura3-52 ash1::kanMX4*	This study
JW1055	*MATα his3::hisG ura3-52 flo11::kanMX4*	This study
JW1032	*MATα his3::hisG ura3-52 ash1::kanMX4 khd1::kanMX4*	This study
JW1026	*MATα his3::hisG ura3-52 flo11::kanMX4 khd1::kanMX4*	This study
L6902	*MATa/α FLO11::HA/FLO11::HA his3::hisG/his3::hisG ura3-52/ura3-52*	Fink laboratory collection
JW214	*MATa/α FLO11::HA/FLO11::HA his3::hisG/his3::hisG ura3-52/ura3-52 khd1::kanMX4/khd1::kanMX4*	This study
JW364	*MATa/α FLO11::HA/FLO11::HA his3::hisG/his3::hisG ura3-52/ura3-52 ash1::kanMX4/ash1::kanMX4*	This study
JW1045	*MATa/α FLO11::HA/FLO11::HA his3::hisG/his3::hisG ura3-52/ura3-52 ash1::kanMX4/ash1::kanMX4 khd1::kanMX4/khd1::kanMX4*	This study
JW295	*MATα his3::hisG trp1::hisG leu2::hisG ura3-52 KHD1-TAP::HIS3*	This study
JW700	*MATα his3::hisG trp1::hisG leu2::hisG ura3-52 KHD1-TAP::HIS3* P_{FLO11}*::URA3*	This study
JW248	*MATα his3::hisG trp1::hisG leu2::hisG ura3-52 KHD1-TAP::HIS3* P_{FLO11}*::GFP::ADH1 3' UTR::URA3*	This study
JW715	*MATα his3::hisG trp1::hisG leu2::hisG ura3-52 KHD1-TAP::HIS3 FLO11::ADH1 3' UTR::URA3*	This study
JW1239	*MATa his3::hisG ura3-52 KHD1-TAP::HIS3 flo11::natNT2::*P_{ADH}*::FLO11 repeats::GFP::ADH1 3' UTR::URA3*	This study
JW1255	*MATa his3::hisG ura3-52 KHD1-TAP::HIS3 flo11::natNT2::*P_{ADH}*::GFP::ADH1 3' UTR::URA3*	This study
JW1778	*MATa his3::hisG ura3-52 KHD1-TAP::HIS3 flo11::natNT2::*P_{CYC1}*::GFP::ADH1 3' UTR::URA3*	This study
JW1226	*MATa his3::hisG ura3-52 flo11::natNT2::*P_{ADH}*::FLO11 repeats::GFP::ADH1 3' UTR::URA3*	This study
JW1245	*MATa his3::hisG ura3-52 khd1::kanMX4 flo11::natNT2::*P_{ADH}*::FLO11 repeats::GFP::ADH1 3' UTR::URA3*	This study
JW1547	*MATa his3::hisG ura3-52 flo11::natNT2::*P_{ADH}*::GFP::ADH1 3' UTR::URA3*	This study
JW1564	*MATa his3::hisG ura3-52 flo11::natNT2::*P_{ADH}*::GFP::ADH1 3' UTR::URA3 khd1::kanMX4*	This study
JW1549	*MATa his3::hisG ura3-52 flo11::natNT2::*P_{CYC1}*::GFP::ADH1 3' UTR::URA3*	This study
JW1566	*MATa his3::hisG ura3-52 flo11::natNT2::*P_{CYC1}*::GFP::ADH1 3' UTR::URA3 khd1::kanMX4*	This study
JW1330	*MATα his3::hisG ura3-52 natNT2::*P_{ADH}*::FLO11*	This study
JW1430	*MATα his3::hisG ura3-52 natNT2::*P_{ADH}*::FLO11 khd1::kanMX4*	This study

Plasmid	Insert	Source
p413TEF		Mumberg et al. 1995
p413TEF-*KHD1*	*KHD1*	This study
yEGFP3::ADH1 3' UTR::*URA3*		Sherwin Chan

TABLE S2

Oligonucleotides used in this study

Name	Sequence (5' to 3')	Description
JW4	caaacttgctgagtccatgc	amplify *KHD1-TAP::HIS3*
JW5	cgcgaaatgtttaaagcaag	amplify *KHD1-TAP::HIS3*
JW17	tggtcatcctgtaggtttgttg	amplify *khd1::kanMX4*
JW18	cagttctgccgggatacagt	amplify *khd1::kanMX4*
JW39	cgtgcgtctgatttctacga	amplify *ash1::kanMX4*
JW44	aagcaggttccgctatttca	amplify *ash1::kanMX4*
JW46	aattgggattcaaggcatca	amplify *flo11::kanMX4*
JW47	aattgggattcaaggcatca	amplify *flo11::kanMX4*
JW48	aaggaaaaaagcggccgctggtcatcctgtaggtttgttg	clone *KHD1*
JW49	atatatccgctcgagcgttgtattgttgttcggattg	clone *KHD1*
JW176	taattaagaatatacttttgtaggcctcaaaaatccatatacgcacactatgcgtacgctgcaggtcgac	P_{ADH}/P_{CYC1} amplification
JW186	caattgttgtcacaatctatgttccaatagaagcctgggaaatctgtttgcatcgatgaattctctgtcg	P_{ADH} fused to *FLO11* repeats
JW218	tcaaccaaaattgggacaacaccagtgaataattcttcacctttagacat-catcgatgaattctctgtcg	P_{CYC1} fused to *GFP*
JW228	aatgatacggcgaccaccgacagagggaggacgatgcgg	CLIP RT-PCR
JW229	caagcagaagacggcatacgaccgctggaagtgactgacac	CLIP RT-PCR
JW230	cgacagagggaggacgatgcgg	Illumina sequencing
FLO11 FW	cacttttgaagtttatgccacacaag	*FLO11* qPCR
FLO11 RV	cttgcatattgagcggcactac	*FLO11* qPCR
ACT1 FW	ctccaccactgctgaaagagaa	*ACT1* qPCR
ACT1 RV	ccaaggcgacgtaacatagtttt	*ACT1* qPCR
Vla292	cactggtgttgtcccaattttg	*GFP* qPCR
Vla293	caccggagacagaaaatttgtg	*GFP* qPCR
JW348	aggaggacgcggctaataatta	*TUB1* qPCR
JW349	tcgcccaaaatttctctacca	*TUB1* qPCR

TABLE S3

CLIP peaks

Table S3 is available for download as an Excel file at http://www.genetics.org/cgi/content/full/genetics.110.113944/DC1.

TABLE S4

Khd1 target RNAs

Table S4 is available for download as an Excel file at http://www.genetics.org/cgi/content/full/genetics.110.113944/DC1.